Investigation of germanium quantum-well light sources

Edward T. Fei,[1,4] Xiaochi Chen,[1,4] Kai Zang,[1] Yijie Huo,[1,*] Gary Shambat,[1] Gerald Miller,[2] Xi Liu,[3] Raj Dutt,[2] Theodore I. Kamins,[1] Jelena Vuckovic,[1] and James S. Harris[1]

[1] *Department of Electrical Engineering, Stanford University, Stanford, CA 94305, USA*
[2] *APIC Corporation, 5800 Uplander Way, Suite 200, Culver City, CA 90230, USA*
[3] *Department of Materials Science, Stanford University, Stanford, CA 94305, USA*
[4] *The first two authors contributed equally to this work*
[*] *yjhuo@stanford.edu*

Abstract: In this paper, we report a broad investigation of the optical properties of germanium (Ge) quantum-well devices. Our simulations show a significant increase of carrier density in the Ge quantum wells. Photoluminescence (PL) measurements show the enhanced direct-bandgap radiative recombination rates due to the carrier density increase in the Ge quantum wells. Electroluminescence (EL) measurements show the temperature-dependent properties of our Ge quantum-well devices, which are in good agreement with our theoretical models. We also demonstrate the PL measurements of Ge quantum-well microdisks using tapered-fiber collection method and quantify the optical loss of the Ge quantum-well structure from the measured PL spectra for the first time.

OCIS codes: (200.4650) Optical interconnects; (250.5590) Quantum-well, -wire and -dot devices; (250.5230) Photoluminescence; (230.3670) Light-emitting diodes; (210.4590) Optical disks; (310.1860) Deposition and fabrication.

References and links

1. C. A. Mack, "Fifty years of Moore's law," IEEE Trans. Semicond. Manuf. **24**(2), 202–207 (2011).
2. M. T. Bohr, "Interconnect scaling-the real limiter to high performance ULSI," in *International Electron Devices Meeting* (IEDM, 1995), pp. 241–244.
3. E. Fei, E. Edwards, Y. Huo, X. Chen, S. Claussen, X. Liu, Y. Rong, T. Kamins, D. Miller, and J. S. Harris, "Low power SiGe electroabsorption modulators for optical interconnects," in *Advanced Photonics Congress*, OSA Technical Digest (online) (OSA, 2012), paper IM4A.3.
4. Y. Kang, H.-D. Liu, M. Morse, M. J. Paniccia, M. Zadka, S. Litski, G. Sarid, A. Pauchard, Y.-H. Kuo, H.-W. Chen, W. S. Zaoui, J. E. Bowers, A. Beling, D. C. McIntosh, X. Zheng, and J. C. Campbell, "Monolithic germanium/silicon avalanche photodiodes with 340 GHz gain–bandwidth product," Nat. Photonics **3**(1), 59–63 (2009).
5. S.-L. Cheng, J. Lu, G. Shambat, H.-Y. Yu, K. Saraswat, J. Vuckovic, and Y. Nishi, "Room temperature 1.6 microm electroluminescence from Ge light emitting diode on Si substrate," Opt. Express **17**(12), 10019–10024 (2009).
6. P. Chaisakul, D. Marris-Morini, G. Isella, D. Chrastina, N. Izard, X. Le Roux, S. Edmond, J.-R. Coudevylle, and L. Vivien, "Room temperature direct gap electroluminescence from Ge/$Si_{0.15}Ge_{0.85}$ multiple quantum well waveguide," Appl. Phys. Lett. **99**(14), 141106 (2011).
7. J. Xia, Y. Takeda, N. Usami, T. Maruizumi, and Y. Shiraki, "Room-temperature electroluminescence from Si microdisks with Ge quantum dots," Opt. Express **18**(13), 13945–13950 (2010).
8. J. Liu, X. Sun, R. Camacho-Aguilera, L. C. Kimerling, and J. Michel, "Ge-on-Si laser operating at room temperature," Opt. Lett. **35**(5), 679–681 (2010).
9. R. E. Camacho-Aguilera, Y. Cai, N. Patel, J. T. Bessette, M. Romagnoli, L. C. Kimerling, and J. Michel, "An electrically pumped germanium laser," Opt. Express **20**(10), 11316–11320 (2012).
10. H. K. Choi and C. A. Wang, "InGaAs/AlGaAs strained single quantum well diode lasers with extremely low threshold current density and high efficiency," Appl. Phys. Lett. **57**(4), 321–323 (1990).
11. S. Galdin, P. Dollfus, V. Aubry-Fortuna, P. Hesto, and H. J. Osten, "Band offset predictions for strained group IV alloys: $Si_{1-x-y}Ge_xC_y$ on Si (001) and $Si_{1-x}Gex$ on $Si_{1-z}Gez$ (001)," Semicond. Sci. Technol. **15**(6), 565–572 (2000).

#243414 Received 22 Jun 2015; revised 26 Jul 2015; accepted 27 Jul 2015; published 17 Aug 2015

12. M. V. Fischetti and S. E. Laux, "Band structure, deformation potentials, and carrier mobility in strained Si, Ge, and SiGe alloys," J. Appl. Phys. **80**(4), 2234–2252 (1996).
13. C. G. Van de Walle, "Band lineups and deformation potentials in the model-solid theory," Phys. Rev. B Condens. Matter **39**(3), 1871–1883 (1989).
14. C. G. Van de Walle and R. M. Martin, "Theoretical calculations of heterojunction discontinuities in the Si/Ge system," Phys. Rev. B Condens. Matter **34**(8), 5621–5634 (1986).
15. A. Nayfeh, C. O. Chui, K. C. Saraswat, and T. Yonehara, "Effects of hydrogen annealing on heteroepitaxial-Ge layers on Si: surface roughness and electrical quality," Appl. Phys. Lett. **85**(14), 2815 (2004).
16. S. Saitoa, K. Odaa, K. Tania, M. Takahashia, E. Nomotob, T. Okumurab, Y. Suwac, Y. Leed, M. Sagawae, T. Sugawarae, and T. Idoe, "Si/ge quantum well light-emitting diode for monolithic integration in Si photonics chips," E. C. S. Trans. T. E. Soc. **45**(5), 103–112 (2012).
17. K. Gallacher, P. Velha, D. J. Paul, S. Cecchi, J. Frigerio, D. Chrastina, and G. Isella, "1.55 µm direct bandgap electroluminescence from strained n-Ge quantum wells grown on Si substrates," Appl. Phys. Lett. **101**(21), 211101 (2012).
18. X. Chen, Y. Huo, E. T. Fei, G. Shambat, K. Zang, X. Liu, Y. Chen, T. I. Kamins, J. Vuckovic, and J. S. Harris, "A new approach to Ge lasers with low pump power," IEEE Photonics Conference, 60–61 (2012).
19. R. Regener and W. Sohler, "Loss in low-finesse Ti: LiNbO3 optical waveguide resonators," Appl. Phys. B **36**(3), 143–147 (1985).

1. Introduction

In recent years, electronic device speeds have continued to increase with each generation [1]; however, the speed of on-chip communications has not been able to keep pace creating an interconnect bottleneck for chip performance [2]. Switching from electrical to optical interconnects is one possible solution to overcoming this bottleneck, and recent work has demonstrated impressive results in the field of Si-compatible modulators [3] and detectors [4]. However, an integrated light source for such a system is a major challenge and still needs further development. For most of the work in this field, Ge is the material of choice because it is Si compatible and it has a direct bandgap located only slightly above the indirect bandgap at room temperature. In the past few years, electroluminescence has been demonstrated in bulk Ge [5], Ge quantum wells [6] and Ge quantum dots [7]. Furthermore, both optically and electrically pumped bulk Ge lasers [8,9] have been demonstrated. However, the threshold current density of these demonstrated Ge lasers is extremely high due to the low fraction of electrons in the direct bandgap, high Shockley-Read-Hall and Auger recombination rates and the large active volume. On the other hand, quantum-well structures have successfully reduced the thresholds in lasers based on III-V materials [10]. Thus, here we present an investigation of the optical properties of Ge quantum wells including carrier-density simulations, photoluminescence (PL), electroluminescence (EL), temperature dependence and optical loss of the material. To the best of our knowledge, this is the first time Ge quantum-well optical loss has been studied for side-coupled Ge quantum-well microdisks.

2. Simulation

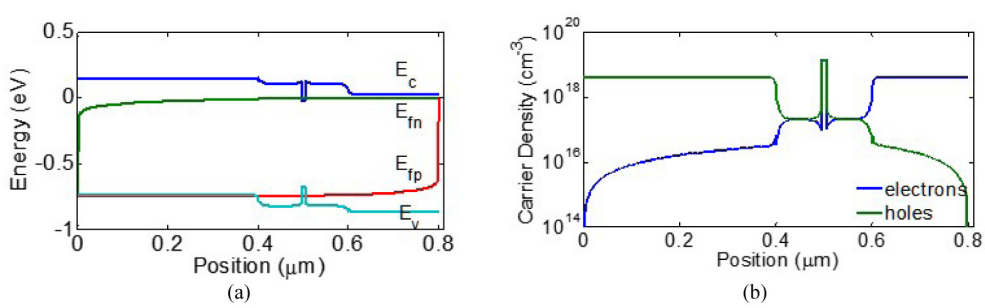

Fig. 1. (a) Sentaurus simulation of the band diagram and quasi-Fermi levels of a Ge quantum-well p-i-n diode under 0.76V forward bias. (b) Sentaurus simulation of carrier density in the same device.

#243414 Received 22 Jun 2015; revised 26 Jul 2015; accepted 27 Jul 2015; published 17 Aug 2015

We carried out Sentaurus simulations of a Ge quantum-well p-i-n diode. In the intrinsic region of the simulated structure, the 10 nm thick Ge quantum well is sandwiched between 100 nm thick $Si_{0.2}Ge_{0.8}$ barriers. The n- and p-type layers are $Si_{0.2}Ge_{0.8}$ with doping concentration of 4×10^{18} cm^{-3}. To mimic the band structure of our fabricated devices, we included the effect of strain in the bandgap and band-offset calculations by assuming that both the Ge and the $Si_{0.2}Ge_{0.8}$ layers are epitaxially grown on a relaxed $Si_{0.1}Ge_{0.9}$ layer [11,12]. Very significantly, although the conduction-band minima of relaxed $Si_{0.2}Ge_{0.8}$ are located in Δ-valleys, strained $Si_{0.2}Ge_{0.8}$ on a relaxed $Si_{0.1}Ge_{0.9}$ layer has its conduction-band minima at *L*-valleys [13,14]. The band diagram in Fig. 1(a) clearly shows that the quasi-Fermi levels are much closer to the band edges in the Ge quantum-well region than in neighboring barrier regions. The carrier concentrations shown in Fig. 1(b) confirm that the quantum well provides strong carrier confinement and that high carrier concentrations can be achieved with relatively low injection current. Further calculations show that the Ge quantum-well structure can have $>10^{19}$ cm^{-3} carriers with only 500 A/cm^2 injection current, whereas a 200 nm bulk Ge device would require at least 7000 A/cm^2 to achieve comparable carrier concentrations.

3. Materials

Our samples were grown on <100> Si wafers in an Applied Materials reduced-pressure (~5-100 Torr) chemical vapor deposition (RPCVD) system using silane and germane as the precursors and arsine and diborane for dopants. The buffer layers were grown using the multiple hydrogen anneal for heteroepitaxy (MHAH) method [15], allowing us to grow high quality (smooth, low dislocation density) films using relatively thin buffers, which allows easier integration of these devices with an on-chip optical network. The material was grown at 405 °C and 40 Torr. After two 200 nm SiGe buffer growth/anneal steps, three strain balanced Ge/SiGe quantum wells were grown, followed by a 200 nm SiGe cap. The entire growth stack is shown in Fig. 2.

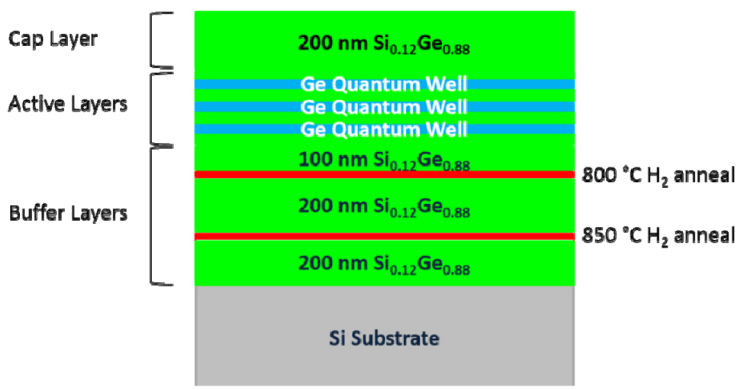

Fig. 2. Growth stack for Ge quantum-well diode.

4. Experimental results

PL measurements were performed using a 532 nm, 25 mW Nd:YAG laser pump. The emissions of the samples were filtered by a 1400 nm long pass filter and detected by an InGaAs detector. We compared the PL intensity between a Ge quantum-well sample and a bulk Ge sample to determine if the quantum-well structure enhances PL. The Ge quantum-well sample has three ~14 nm thick Ge quantum wells separated by ~17 nm thick $Si_{0.19}Ge_{0.81}$ barriers, and the bulk Ge sample has a 200 nm thick Ge film. The two samples were grown on similar $Si_{0.12}Ge_{0.88}$ buffer growth stacks and thus have comparable material quality. The PL results shown in Fig. 3 indicate transition energies of 0.83 eV (~1500 nm) and 0.85 eV (~1460 nm) for the bulk Ge sample and the Ge quantum-well sample, respectively. These

#243414 Received 22 Jun 2015; revised 26 Jul 2015; accepted 27 Jul 2015; published 17 Aug 2015

photon energies imply the photon emission is from the Γ-valley of the Ge material. The cut-off at 1400 nm is due to the long pass filter in the measurement setup. The PL intensity of the quantum-well sample with ~40 nm total Ge thickness is higher than that of the 200 nm thick bulk Ge sample. Due to carrier confinement, a significant enhancement of local electron and hole concentrations is achieved in the Ge quantum wells, as shown in Fig. 1(b). According to the thermal distribution, the ratio of electron concentration in the Γ-valley of the Ge conduction band to the total electron concentration in the Ge is roughly constant as the total electron concentration changes. Thus, the electron concentration in the Γ-valley of the conduction band in the Ge quantum wells is significantly enhanced as well. The radiative recombination rate in the Ge quantum wells is enhanced even more because it is proportional to the product of the excess electron concentration in the Γ-valley of the conduction band and the excess hole concentration in the valence band. As a result, although the total thickness of the Ge quantum wells is much less than the thickness of the bulk Ge, the PL intensity of the quantum-well sample is higher than that of the bulk Ge sample. Also, a slight blue-shift in the emission peak can be observed and is due to quantum confinement and residual unrelaxed compressive strain.

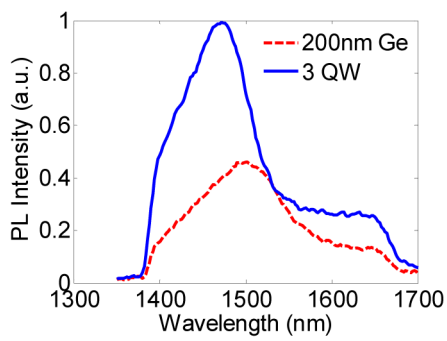

Fig. 3. Photoluminescence of Ge quantum wells and thick Ge film.

We also performed power-dependent EL measurements of Ge quantum-well devices and the observed results are consistent with previously reported measurements [6,16,17]. We saw super-linear behavior of EL intensity, as well as a red-shift in the emission peak at higher injection currents. For EL intensity fitting, in addition to the temperature dependence of the thermal distribution considered in [6], we believe the temperature dependence of the energy separation between Γ and L valleys, $\Delta E_{\Gamma L}$, should play an important role. Therefore, we conducted temperature-dependent measurements to further investigate these phenomena. For our temperature-dependent measurements, the device was operated with a constant current density of 250 A/cm^2 while we varied the temperature of a heating stage beneath the device as we took EL spectra. The results shown in Fig. 4 confirm that heating alone can cause both a red-shift and higher EL intensity. Further investigation into the emission wavelength shows that the overall red-shift is primarily caused by the temperature dependence of the Ge direct bandgap which causes a red-shift according to $E_\Gamma = 0.89\text{-}5.82 \times 10^{-4} \times T^2/(T + 296)$ eV, as well as the thermal change in carrier distribution which causes a slight offsetting blue-shift. We compared our measured results to theoretical predictions of the emission wavelength based on those effects with a correction for material strain and quantum confinement, and we found the results and the predictions to be in good agreement as shown in Fig. 5(a). Also, we found that the higher EL intensity can be attributed to an increased carrier concentration in the Γ-valley because of the temperature-dependent thermal distribution and temperature-dependent $\Delta E_{\Gamma L}$. We calculated the predicted effect on EL intensity due to the two temperature-dependent effects using the equation $A \times \exp(-\Delta E_{\Gamma L}(T)/kT)$, where $\Delta E_{\Gamma L}(T)$ is the

#243414 Received 22 Jun 2015; revised 26 Jul 2015; accepted 27 Jul 2015; published 17 Aug 2015

energy difference between the L-valley and the Γ-valley in the conduction band as a function of T, and found it to be in good agreement with measured results, as shown in Fig. 5(b).

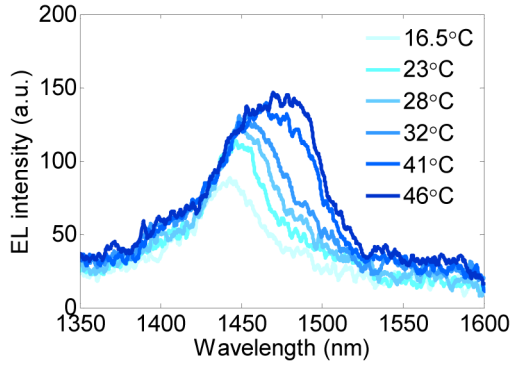

Fig. 4. Temperature-dependent EL spectra for Ge quantum-well diode operating under 250 A/cm^2 injection current.

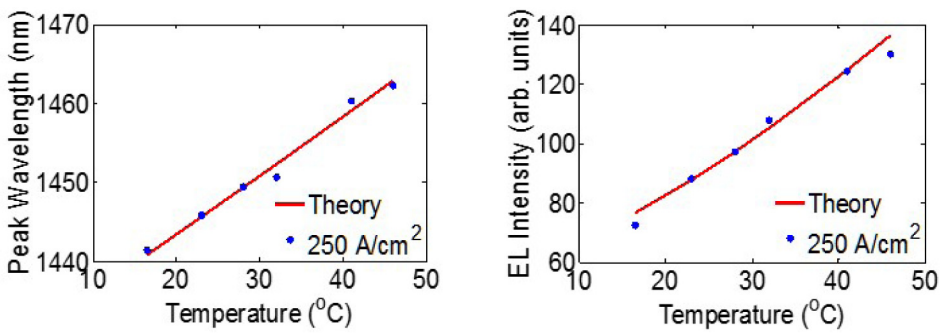

(a) (b)

Fig. 5. (a) Emission wavelength as a function of temperature for Ge quantum-well diode. The red line shows the theoretical shift expected for this material. (b) Temperature dependence of EL intensity for Ge quantum-well diode. The red line shows the predicted change in EL intensity.

We also calculated the optical loss in the Ge quantum wells by measuring the PL of microdisk structures. The microdisks were patterned by standard optical lithography and dry etched ~1.4 μm [18]. A scanning electron microscope (SEM) image of the device is shown in Fig. 6(a). The Ge quantum well thickness (~10 nm) of this Ge quantum-well sample is less than those used for the PL and EL measurements reported above. We were able to measure the PL of the resonant modes using the tapered-fiber collection method shown in Fig. 6(b). For these measurements, the sample was pumped from the top using a 980 nm laser operating in continuous-wave mode with varying power. The resulting PL shown in Fig. 7(a) was collected through the fiber and shows clear resonant modes of the microdisk being excited.

#243414 Received 22 Jun 2015; revised 26 Jul 2015; accepted 27 Jul 2015; published 17 Aug 2015

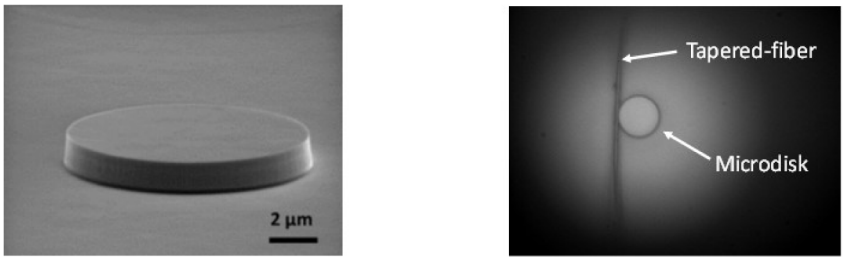

(a) (b)

Fig. 6. (a) Scanning electron microscopy of a Ge quantum-well microdisk. (b) Top-view optical micrograph of measurement geometry for Ge quantum-well microdisk. The micodisk is pumped vertically and the coupled fiber extracts the output light from the sides of the microdisk.

We define the optical loss to be the sum of the loss from direct transitions, the loss from free carrier absorption and the loss from sidewall scattering. We calculated the upper limit of the optical loss as a function of wavelength and pump power using the method proposed in [19]. Although this method was originally proposed for Fabry-Perot waveguide resonators, it can also be applied to microdisk resonators if we consider the transmissivity T to be equivalent to the fiber coupling coefficient and the mode reflectivity R to be 1. Following the derivation in [19], we relate the optical loss to the contrast by

$$\alpha = -\frac{\ln\left[\frac{1}{K}\left(1-\sqrt{1-K^2}\right)\right]}{2\pi r} \tag{1}$$

where

$$K = \frac{I_{\max} - I_{\min}}{I_{\max} + I_{\min}} \tag{2}$$

is the contrast of the resonances. With these equations, we were able to extract the optical losses at different wavelengths from the PL spectra, with the results shown in Fig. 7(b).

Compared to the optical loss at 1530 nm, the optical loss at 1400 nm is decreased by 630 cm^{-1} at a pump intensity of 10 mW. We attribute this to the decreased loss from direct transitions at 1400 nm since the free carrier absorption and sidewall scattering loss are not very sensitive to wavelength in this wavelength range. Furthermore, by comparing the optical losses at pump intensities of 10 mW and 60 mW, we find that the loss from direct transitions can decrease by a further 350 cm^{-1} at 1400 nm as the pump intensity is increased from 10 mW to 60mW. This is a conservative estimate considering that the free carrier absorption at the pump intensity of 60 mW is higher than that at the pump intensity of 10 mW.

#243414 Received 22 Jun 2015; revised 26 Jul 2015; accepted 27 Jul 2015; published 17 Aug 2015

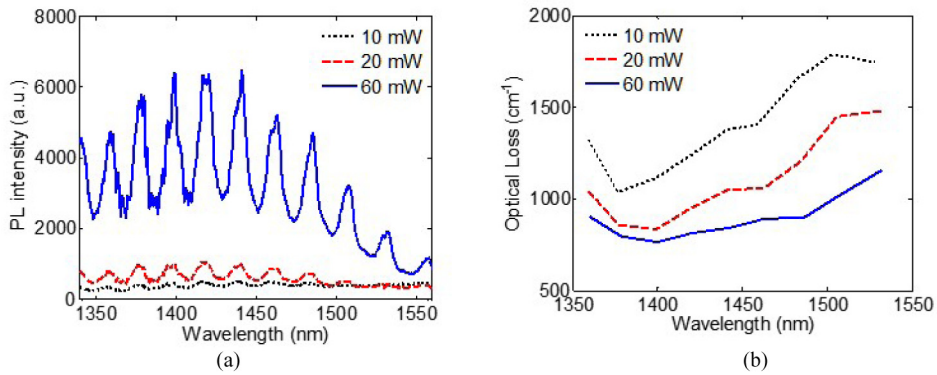

Fig. 7. (a) Photoluminescence results from a Ge quantum well microdisk at varying pump powers. (b) Optical loss for the Ge quantum well microdisk calculated from Fig. 7(a).

5. Conclusion

In this paper, we have reported the results of a broad investigation of the optical properties of Ge quantum-well devices grown on Si substrates using a thin MHAH buffer. Through simulations and PL measurements, we have shown increased carrier densities and enhanced direct-bandgap PL from Ge quantum wells at room temperature. Furthermore, our study of the temperature dependence of our Ge quantum-well diode shows that we can successfully predict the EL peak wavelengths and intensities of our devices based on the models presented. Finally, our PL measurements of Ge quantum-well microdisks allow us to quantify the optical loss of Ge quantum wells for the first time. These results are crucial in understanding the challenges and designing future Ge quantum-well devices for efficient light emission, thus bringing us one step closer to achieving a high-efficiency light source for on-chip optical interconnects.

#243414 Received 22 Jun 2015; revised 26 Jul 2015; accepted 27 Jul 2015; published 17 Aug 2015